# Experimental Study on Triaxial Geogrid-Reinforced Bases over Weak Subgrade under Cyclic Loading

Yu Qian [1], Jie Han[2], Sanat K. Pokharel[3], and Robert L. Parsons[4]

[1]M.S. student, Research Assistant, Department of Civil, Environmental, and Architectural Engineering, the University of Kansas, Lawrence, Kansas 66045, USA; email: qiany0905@ku.edu
[2]Ph.D., PE, Associate Professor, Department of Civil, Environmental, and Architectural Engineering, the University of Kansas, Lawrence, Kansas 66045, USA; email: jiehan@ku.edu
[3]Ph.D. candidate, Research Assistant, Department of Civil, Environmental, and Architectural Engineering, the University of Kansas, Lawrence, Kansas 66045, USA; email: sanpok@ku.edu
[4]Ph.D., PE, Associate Professor, Department of Civil, Environmental, and Architectural Engineering, the University of Kansas, Lawrence, Kansas 66045, USA; email: rparsons@ku.edu

## ABSTRACT

Geogrids have been successfully used to improve soft subgrade and reinforce weak base course by providing lateral confinement. However, uniaxial and biaxial geogrids cannot provide uniform resistance in all directions. A new product termed "Triaxial geogrid" was developed to overcome this limitation. The triaxial geogrid is expected to have a more stable grid structure to provide uniform resistance in all directions as compared with uniaxial and biaxial geogrids. However, the effects of the triaxial geogrids on the performance of reinforced bases have not been well evaluated. In this study, unreinforced and triaxial geogrid-reinforced bases over a weak subgrade were constructed in a large geotechnical testing box (2m x 2.2m x 2m high) at the University of Kansas and tested under cyclic loading. During the tests, the surface deformations and the vertical stresses at the interface between the base and the subgrade were monitored. The test results showed that triaxial geogrids increased percentage of resilient displacement and reduced permanent displacement and vertical stresses at the interface as compared with the unreinforced base.

## INTRODUCTION

Geosynthetics have been successfully used for subgrade improvement and base reinforcement for unpaved and paved roads in the past several decades. Many studies have shown that a geosynthetic properly placed in a roadway does improve the performance of the road. Das et al. (1998) pointed out that the most effective location of the geosynthetic for subgrade improvement is at the interface between the selected granular material and the subgrade. In this location the geosynthetic provides separation, lateral restraint of the overlying granular material, and a tensioned membrane effect when deformed extensively. Geotextiles and geogrids are two main types of geosynthetics commonly used in unpaved roads. However, there is a significant difference between geotextiles and geogrids. Nonwoven geotextiles are mainly used for separation and drainage; woven geotextiles are used for separation and reinforcement; and geogrids are typically used for confinement and reinforcement. The confinement due to the geogrid increases the modulus of the base course, which leads to a wider vertical stress distribution over the subgrade and consequently a reduction of vertical subgrade deformation (Love 1984; Hass et al 1988). Due to their apertures, geogrids can interlock with the aggregates in the base course if there is an appropriate relationship between the aperture size of the geogrid and the particle size of the aggregate (Giroud and Han 2004a, b). The reduction in the shear stress on the subgrade interface can reduce the subgrade deformation (Perkins 1999).

In the past, geogrids could be classified into being uniaxial and biaxial. As Dong et al. (2010) demonstrated, biaxial geogrids cannot provide uniform tensile stiffness and strengths in different directions. The uniaxial geogrids have stiffness and strength in one direction. A new product termed “triaxial geogrid” was developed to overcome this limitation. Since the triaxial geogrid has a more stable grid structure, it is expected to provide uniform tensile stiffness and strength in all directions as compared with uniaxial and biaxial geogrids. However, the effects of the triaxial geogrids on the performance of reinforced bases have not been well evaluated.

This study investigated the performance of triaxial geogrid-reinforced bases over weak subgrade under cyclic loading. A set of laboratory tests were conducted to investigate the influence of triaxial geogrids on the reduction in the permanent deformations and the vertical stresses at the interface between the base and the subgrade as compared with unreinforced bases.

## MATERIALS

Two triaxial geogrids (named as TX1 and TX2), made of polypropylene, were used in this experimental study. The index properties of these two triaxial geogrids are present in Table 1. TX2 geogrid is stronger than TX1 geogrid.

AB3 aggregate, commonly adopted in Kansas, was used as a base course material. This material has the following physical properties: specific gravity ($G_s$) =2.69, liquid limit (LL) =20, plastic limit (PL) =13, mean particle size ($d_{50}$) =7.0 mm, coefficient of uniformity ($C_u$) =133, and coefficient of curvature ($C_c$) =2.25. The grain size distribution of AB3 is presented in Figure 1. The optimum moisture content of this aggregate is 10.0%. To examine the effect of the base course stiffness, the base courses were compacted to achieve two California Bearing Ratios (CBR) at approximately 5% and 20%. The CBR values were estimated by the dynamic cone penetrometer (DCP) penetration indices after the preparation of the base course. Due to the page limit, this paper presents the test results based on the base course at CBR of

5%. The test results based on the base course at the CBR of 20% will be presented in future publications.

**Table 1 Index Properties of Two Triaxial Geogrids**

| Index Properties | Longitudinal | | Diagonal | | Transverse | | General | |
|---|---|---|---|---|---|---|---|---|
| | TX1 | TX2 | TX1 | TX2 | TX1 | TX2 | TX1 | TX2 |
| Rib pitch (mm) | 40 | 40 | 40 | 40 | | | | |
| Mid-rib depth (mm) | | | 1.8 | 2.3 | 1.5 | 1.8 | | |
| Mid-rib width (mm) | | | 1.1 | 1.2 | 1.3 | 1.3 | | |
| Nodal thickness (mm) | | | | | | | 3.1 | 4.1 |
| Rib shape | | | | | | | rectangular | rectangular |
| Aperture shape | | | | | | | triangular | triangular |

The weak subgrade was an artificial soil composed of a mixture of 75 percent Kansas River sand and 25 percent kaolinite by weight. The grain size distribution of Kansas River sand is presented in Figure 1. Compaction tests were performed to obtain the compaction curve for this subgrade as shown in Figure 2. The maximum dry density is 2.01g/cm$^3$, which corresponds to the optimum moisture content of 10.8%. A series of laboratory un-soaked CBR tests (ASTM D 1188) for the subgrade were performed at different water contents. The CBR vs. moisture content curve is presented in Figure 3. The subgrade soil was compacted at a water content of 11.4% for the box tests to achieve its CBR at approximately 2%, which were verified by vane shear tests and DCP tests.

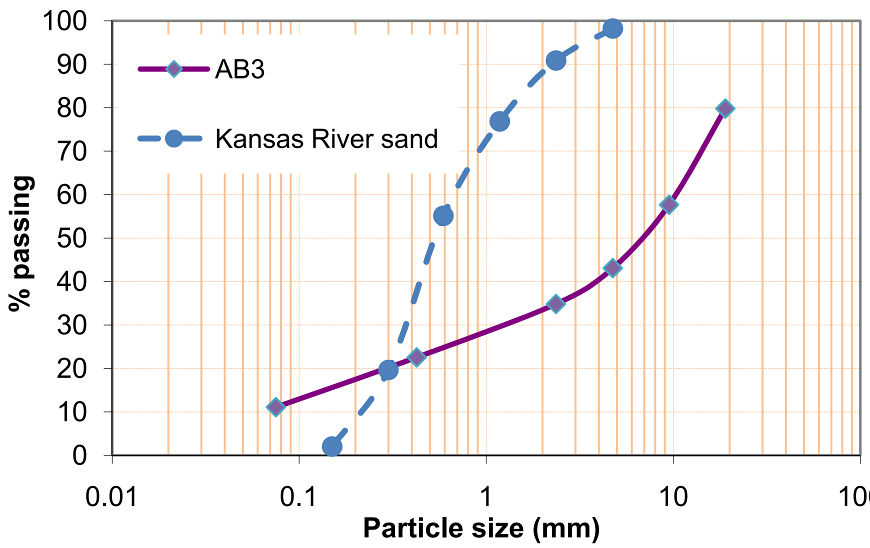


**Figure 1. Grain size distribution curves of Kansas River sand (Han et al. 2008) and AB 3 aggregate**

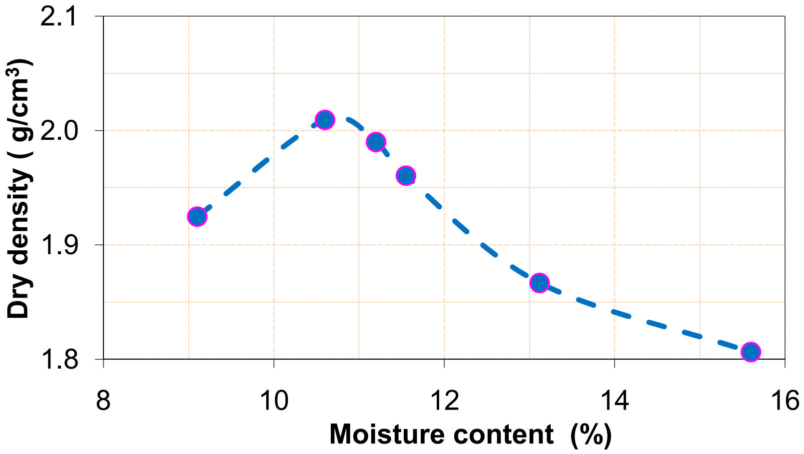


**Figure 2. Compaction curve of the subgrade**

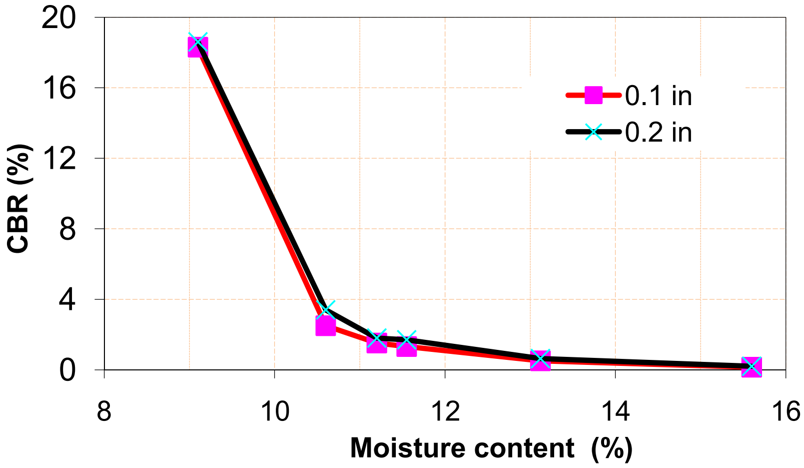


**Figure 3. CBR vs. moisture content of the subgrade**

## TEST SETUP

Cyclic plate loading tests were conducted in a large test box system in the geotechnical laboratory at the Department of Civil, Environmental, and Architectural Engineering at the University of Kansas. This system includes a loading actuator, a data acquisition system, and a steel box (2 m x 2.2 m x 2 m high).

The loading system was an MTS hydraulic loading system. The steel loading plate had a diameter of 0.3 m. For both unreinforced and reinforced bases, cyclic loading tests were conducted. The cyclic loading waves were generated with a peak force of 40 kN and a trough force of 0.5 kN as shown in Figure 4. The frequency of this wave was 0.77 Hz. The peak load was selected to simulate a single wheel load of 40 kN (equal to an axle load of 80kN and a contact pressure of 550 kPa).

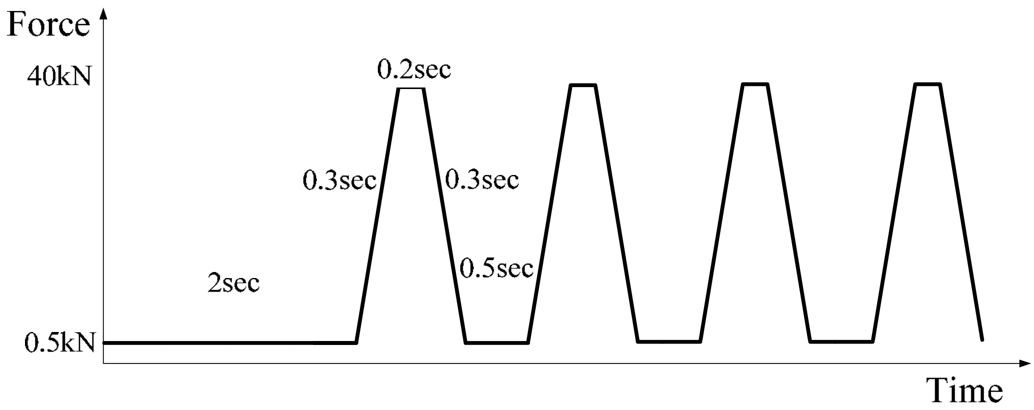


**Figure 4. Cyclic loading wave**

The instrumentation and data acquisition system included four earth pressure cells, five displacement transducers, and two piezometers. Details of the test box system and the reinforced section are illustrated in Figure 5 as an example.

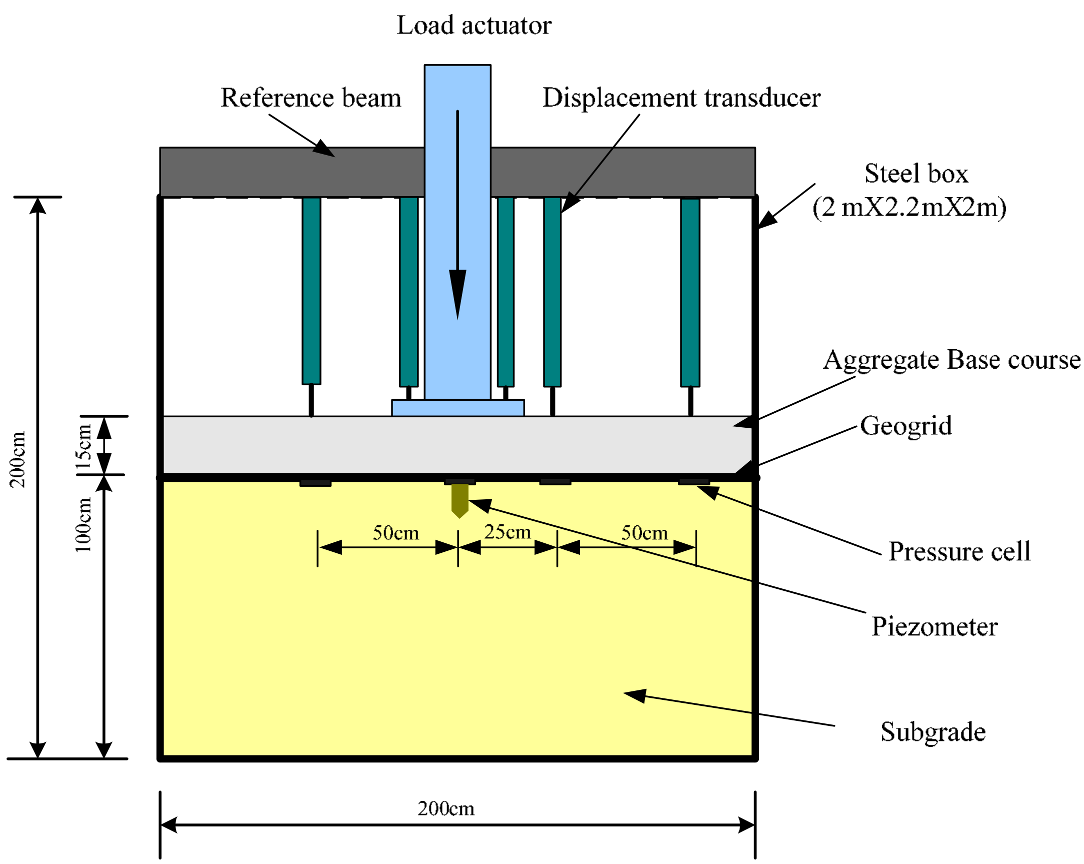


**Figure 5. Setup of a cyclic plate loading test**

The subgrade was placed and compacted in four layers (150 mm thick for each layer) at the moisture content of 11.4% for the top 600 mm subgrade. The base course was compacted to a thickness of 150 mm at the moisture content of 8.9%. The triaxial geogrid was placed at the interface between the subgrade and the base course.

## RESULTS AND DISCUSSION

In this study, the performance of triaxial geogrids in reinforced base courses (CBR=5%) over weak subgrade (CBR=2%) was investigated. A permanent displacement of the loading plate at 75mm was used as the criteria to terminate the cyclic loading test. Figure 6 presents the permanent displacement of the loading plate versus the number of loading cycles for the unreinforced and reinforced bases by TX1 and TX2 geogrids. It is shown that the permanent displacements for all the bases are similar for the initial few cycles because the geosynthetic reinforcement did not take effect at small displacements. With an increase of the number of loading cycles, the benefit of geogrids became more obvious and the base with the stronger geogrid (TX2) had much lower permanent displacements than those of the unreinforced base and the one with the weaker geogrid (TX1). It is expected that the benefit of TX geogrids would become more significant if a stiffer base course were used. The numbers of cycles for the unreinforced, TX1, and TX2-reinforced bases at the permanent displacement of 75 mm were 14, 22, and 32 respectively. Therefore, the improvement factors for TX1 and TX2 geogrids, defined as the ratio of the number of cycles for the reinforced base to that for the unreinforced base at the permanent displacement of 75 mm, were 1.6 and 2.3, respectively.

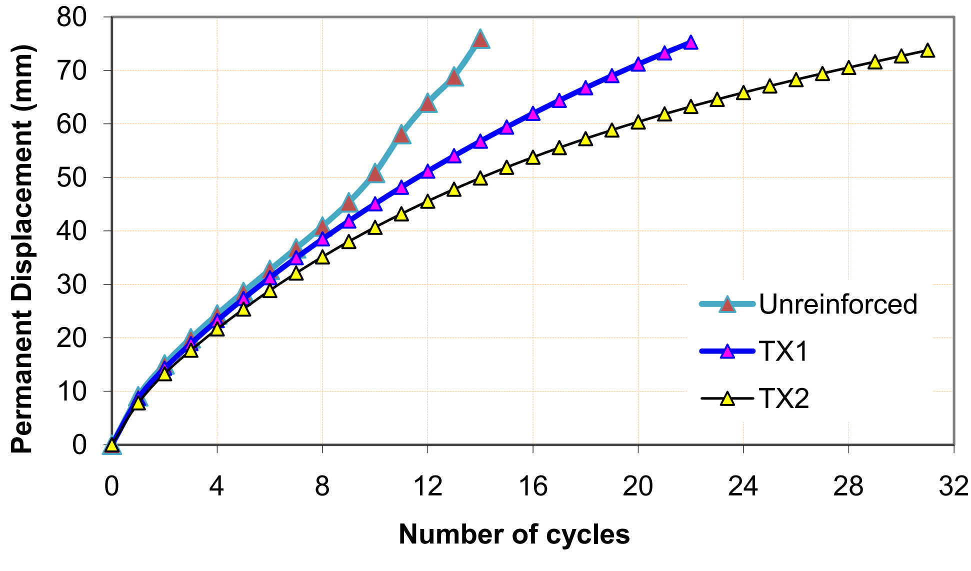


**Figure 6. Permanent displacement of the loading plate versus the number of cycles**

Figure 7 presents the percentage of resilient displacement at each loading cycle for the unreinforced or reinforced base by TX1 or TX2. The percentage of resilient displacement was calculated as the rebound divided by the total displacement in each cycle. It can be seen that the percentage of resilient displacement increased nearly linearly for both reinforced bases up to 60 to 80%. The TX geogrids significantly increased the percentage of resilient displacement as compared with the unreinforced base. In other words, the reinforced bases are more resilient than the unreinforced base.

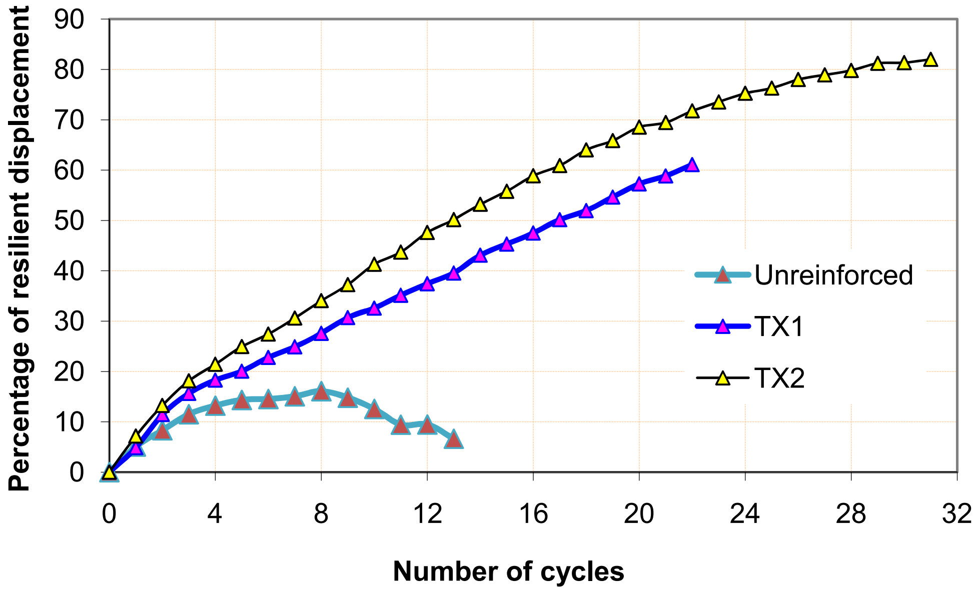


**Figure 7. Percentage of resilient displacement of the loading plate versus the number of cycles**

Figure 8 presents the measured maximum vertical stress at the interface between the base course and the subgrade, which was located along the center of the loading plate. The test results show that the unreinforced base had the highest maximum vertical stress, which is followed by the TX1 and TX2-reinforced bases. The lower maximum vertical stresses in the reinforced bases are attributed to the benefit of the TX geogrids on increasing the stress distribution angle. The TX2 geogrid had a larger distribution angle than the TX1 geogrid. Figure 8 also shows that the maximum vertical stress increased with the number of cycles, which is in good agreement with the finding by Gabr (2001). The increase in the maximum vertical stress with the number of cycles was explained by Giroud and Han (2004a) as the reduction of the stress distribution angle due to the deterioration of the base course. The absolute maximum vertical stresses at the center of the interface were 313, 186, and 103 kPa for the unreinforced, TX1, and TX2-reinforced bases, respectively. It is also found in Figure 8 that the maximum vertical stress decreased slightly after reaching the peak (at the permanent displacement of 70 mm for TX1 and 61 mm for TX2) for both reinforced bases, especially for the TX2-reinforced base. This reduction may result from the tensioned membrane effect of the geogrid at large displacements. Typically, the tensioned membrane effect influences the performance of the reinforced base at a large displacement, such as 100 mm or more (Giroud and Han, 2004b). However, such an effect may become influential at a displacement smaller than 100 mm when the base course is thin (for example, 15cm in this study).

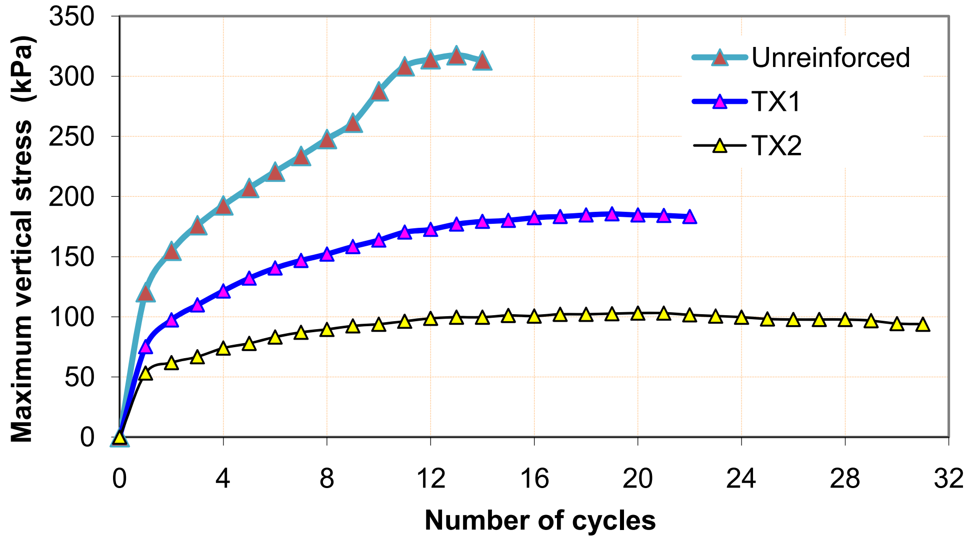


**Figure 8. Maximum vertical stress at the interface between the base and the subgrade**

## CONCLUSIONS

This paper presents experimental results on unreinforced and triaxial geogrid-reinforced bases over weak subgrade under cyclic loading. The following conclusions can be drawn from this study:

1. Triaxial geogrids improved the performance of the reinforced base course over the weak subgrade as compared with the unreinforced base. The improvement factors for TX1 and TX2 geogrids were 1.6 and 2.3, respectively, at the base CBR of 5% over the subgrade CBR of 2%. It is expected that more benefit would be obtained if a base course with a higher CBR were used.
2. The triaxial geogrid-reinforced bases had a higher percentage of resilient displacements than the unreinforced base. The percentage of resilient displacements increased nearly linearly with the number of cycles for the reinforced bases.
3. Triaxial geogrids significantly reduced the maximum vertical stresses at the center of the interface between the base course and the subgrade.
4. The performance of the reinforced-base depended on the type of geogrid. The stronger triaxial geogrid had more contribution to the improvement of the performance.

## ACKNOWLEDGMENTS

This research project was sponsored by Tensar International, Inc. Mr. Joseph Cavanaugh, the vice-president of technology development and Mr. Nicholas Reck, the manager of technology development at Tensar, have provided great help and technical guidance to this study. Mr. Howard Jim Weaver, the lab supervisor in the Department of Civil, Environmental, and Architectural Engineering (CEAE) at the University of Kansas (KU), designed, fabricated, and installed the loading system used for this study. Mr. Milad Jowkar, an undergraduate student in the CEAE Department at KU, provided great assistance to the laboratory tests. The support of all of the above is greatly appreciated.

## REFERENCES

Das, B.M. and Shin, E.C. (1998). "Strip foundation on geogrid-reinforced clay: behavior under cyclic loading." *Geotextiles and Geomembranes*, 13(10): 657-666.

Dong, Y.-L., Han, J., and Bai, X.-H. (2010). "A numerical study on stress-strain responses of biaxial geogrids under tension at different directions." *Proceedings of Geo Florida 2010*, ASCE Geo-Institute, February 20-24, West Palm Beach Florida.

Gabr, M. (2001). *Cyclic Plate Loading Tests on Geogrid Reinforced Roads*. Research Report to Tensar Earth Technologies, Inc., NC State Univ.

Giroud, J.P. and Noiray, L. (1981). "Geotextile-reinforced unpaved road design." *Journal of Geotech. Engineering,* 107(9): 1233–1254.

Giroud, J.P. and Han, J. (2004a). "Design method for geogrid-reinforced unpaved roads. I: Development of design method." *Journal of Geotechnical and Geoenvironmental Engineering*, 130(8): 775–786.

Giroud, J.P. and Han, J. (2004b). "Design method for geogrid-reinforced unpaved roads. II: Calibration and applications." *Journal of Geotechnical and Geoenvironmental Engineering*, 130(8): 787–797.

Haas, R., Wall, J., and Carroll, R.G. (1988). "Geogrid reinforcement of granular bases in flexible pavements." *Transportation Research Record 1188*: 19-27.

Love, J.P. (1984). *Model Testing of Geogrids in Unpaved Roads*. Doctoral Dissertation, University of Oxford, Oxford, UK.

Perkins, S.W. (1999). "Mechanical response of geosynthetic- reinforced flexible pavements," *Geosynthetics International*, 6(5): 347-382.